JOURNAL OF MATERIALS SCIENCE 33 (1998) 477–486

Determination of porosity of reduced hematite by stereologic methods

J. JANOWSKI, A. SADOWSKI
University of Mining and Metallurgy, Faculty of Metallurgy, Al. Mickiewicza 30, 30-059 Cracow, Poland

W. KRAJ, T. RATAJCZAK
Strata Mechanics Research Institute, Polish Academy of Science, ul. Reymonta 27, 30-059 Cracow, Poland

The stereologic analysis of a solid grain has been applied for determination of its porosity. The investigations were carried out on a natural hematite grain reduced to magnetite at 723 K. Stereologic analysis enabled the porosity of this material to be determined on the basis of independently measured grain contours and volume fractions of grain components: hematite, magnetite and pores. A conformity criterion has been formulated, regarding determination of grain volume on the basis of known densities of components and their measured volume fractions in the grain, and on the basis of weight and apparent grain density measurements. The volume increase accompanying reduction of hematite to magnetite, determined from these independent measurements, was in the range 7–19%. By measuring Feret's diameter, the volume of the convex envelope of the grain increased as a result of phase transformation by about 11%. Simultaneously, the volume of the solid phase was found to decrease by 1.5%. The total porosity of the reduced grain, determined by stereologic analysis amounted to 17.5%; 7.7% of which was related to cracks and large pores, and 9.8% to small pores in the magnetite phase. The porosity value determined by the classical mercury method was approximately the same.

1. Introduction

It is known that the porosity of iron oxides significantly affects the mechanism and kinetics of their reduction [1–5]. It is commonly accepted that swelling of iron-bearing materials, e.g. pellets and sinters, takes place in the early stages of the reduction process. Upon considering the consecutive steps of reduction from hematite to iron, it has been proved that 80% of the volume increase takes place during the reduction of hematite to magnetite [6]. The volume increase brought about by such processes as hematite–magnetite transformation, i.e. transformation from the hexagonal hematite lattice to the cubic magnetite lattice, accompanied by pore formation, amounts to 11% [7, 8] to 16% [9]. Pore formation in this process is rather complex and strongly dependent on the thermodynamic conditions, among which the most important are the temperature and composition of the reducing gases. Pore formation is observed simultaneously with nucleation and growth of a new phase. At temperatures ranging from 600 to 800 K, due to the formation of cracks, primary grains of hematite disintegrate into smaller subgrains. Reduction yields porous layers of magnetite on their surfaces [10, 11]. At higher temperatures, 1100–1200 K, reduction proceeds topochemically at the hematite–magnetite interface. A porous layer of magnetite grows over the non-porous core of the unreacted material. The formation of crystallographically orientated lamellae of magnetite at the interface brings about channel-type porosity within the reduced zone [12, 13].

The phase transformation produces pores with various shapes (spherical or channel-type pores), types (open and closed pores) and sizes. It might be of great technological importance to give their complete description. Open pores with larger sizes facilitate the penetration of reducing species, thereby accelerating the reduction process but at the same time they adversely affect the mechanical strength of the material. On the other hand, the formation of subgrains at lower temperatures expands the reaction front, thus intensifying the transformation process.

It must be realized, however, that the great variety of pore shapes, types and sizes, together with the complex pattern of cracks and fissures, makes detailed analysis and comparison of the available results rather difficult. Application of classical porosimetry for investigation of textural transformation is rather unreliable. However, the classical methods do not provide any information on closed pores, neither are they useful in determining the apparent density of the material after reduction. On the other hand, the results of microscopic analysis of a single grain fracture bears an

0022–2461

error related to site selection as well as to the anisotropy of transformation.

Therefore, an attempt has been made in this work, to adopt other methods for determining the porosity of metallurgical materials. An additional advantage is that the new methods enable determination of other texture-related parameters, such as the volume fraction of grain components.

2. Experimental procedure

For these studies crystalline natural hematite from Minas Gerais, Brasil, was chosen. The results of chemical analyses are listed in Table I. The raw material was crushed and then hematite solids that verged upon spherical shape were selected. Jutting corners of these grains were cut off. Finally, the hematite sample consisted of sphere-like grains 2–3 mm in diameter. All these grains of hematite were compact. Microscopic analysis of the cross-section of the initial grain showed no fissures, pores or intergranular spaces. The porosity of the starting material, determined by the Brunauer–Emmett–Teller (BET) method, was not measurable.

Single step reduction from hematite to magnetite was investigated. Reduction progress was monitored thermogravimetrically, using a Mettler TA-1 thermobalance. Before the experiments each grain was weighed and its Feret's diameter determined. Then, three grains were placed on a perforated platinum plate in the reaction chamber of the thermobalance. The composition of the reducing gas, 3% CO + 97% CO_2, was adjusted empirically to ensure such reduction rates that consecutive steps of the phase transformation could be observed. The flow rate of the reducing gas was constant at a level of $30\,\mathrm{Nl\,h^{-1}}$ under a total pressure of 1.01×10^5 Pa.

The reduction was performed isothermally at a temperature of 723 K. The choice of temperature was based on our earlier results, indicating that hematite reduced at low temperature had the most diversified texture. For the same reason the reduction runs were interrupted at the degree of reduction, $R = 0.95$; 0.97 and 0.95, where R was the weight ratio of oxygen actually removed and the total oxygen to be removed in a stoichiometric reaction. For further stereologic analysis, grains reduced to $R = 0.95$ were chosen.

The porosities of magnetite grains obtained by reduction of hematite were additionally determined by means of a Carlo–Erba mercury porosimeter with an extended range, enabling measurement of pore volumes for pores with radii ranging from 0.0037 to 50 μm. A sample of 20 grains, with diameters of 2–3 mm, was taken for these measurements.

TABLE I Impurities in hematite (specularite) sample (wt % × 100)

Mg	Ca	Si	Al	Ti	Mn	K
1	2	17	3	8	0.4	9

3. Discussion

3.1. Stereologic analysis of grains after reduction

Under identical thermodynamic conditions, reduction of a physically and chemically homogeneous oxide proceeds according to the same mechanism. However, individual grains have specific characteristics that are not detectable by methods directed at bulk analysis. This may be the case for the porosity and density of a material. As it is of great importance to know how variation of these parameters affects the reduction rate, the methods used in this work involve individual grain characteristics.

First of all it was essential to find a proper definition for the reduced grain and its volume after transformation. The possibilities offered by stereologic methods for determining the volume and porosity of a hematite grain after reduction, allowed three definitions of a grain to be distinguished, according to which components the grain consisted of:

1. magnetite, hematite, small pores, large pores;
2. magnetite, hematite, small pores; and
3. magnetite, hematite.

The pores and cracks were treated as two different grain components according to the following criteria:

1. spherical pores with diameters ranging from 0.2 to 3 μm, referred to as small pores; and
2. pores or cracks with diameters of > 3 μm, referred to as large pores.

3.1.1. Description of grains by means of Feret's diameter

One possible way of defining grain size is to determine the width of the grain [14]. The grain width, in a direction, $\vec{n}$, is understood to be a distance, $b(\vec{n})$, between two planes supporting the grain, perpendicular to the direction, $\vec{n}$, in three-dimensional space. Because of the requirements of symmetry, the set of directions makes up one-half of a round polyhedral angle, 2π rad. Feret's diameter of a grain, d_{FE} is calculated as a mean integral of its width

$$d_{\mathrm{FE}} = \frac{1}{2\pi} \int_{2\pi} b(\vec{n})\,\mathrm{d}n \qquad (1)$$

Solution of Equation 1 gives the convex envelope of the grain, i.e. the smallest convex solid surrounding the grain (Fig. 1). The volume of such an envelope is not smaller than that of the grain itself. It becomes equal if the grain is convex. The grain profiles were measured on a co-ordinatemetric table of a microscope with minor divisions of 0.01 mm. The grain width, $B(\phi)$, was determined on the basis of the measured co-ordinates (Fig. 2). At a fixed grain position, six values of the angle ϕ, where ϕ was the angular position of the grain in the co-ordinatemetric x–y plane, were determined every 30° between 0 and 150°. Subsequently, the same grain was turned to another position on the table, forced by the stability conditions.

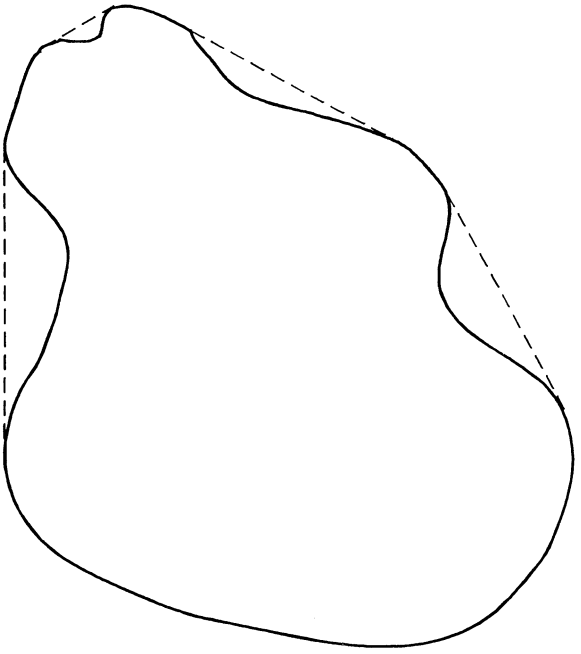

Figure 1 Actual profile of a non-convex grain (—) and its convex envelope (– – –).

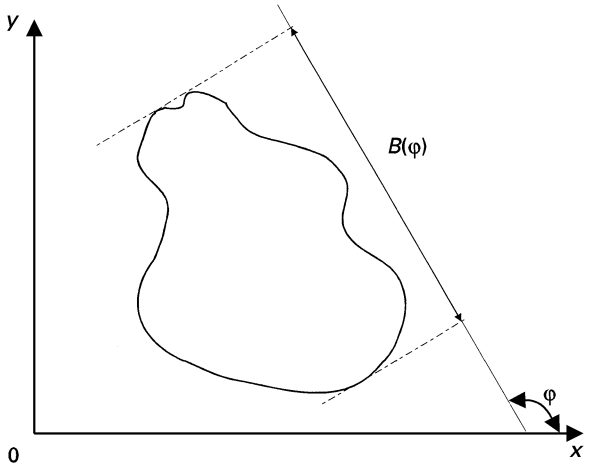

Figure 2 Grain width $B(\varphi)$, in direction n, defined by angle φ relative to x-axis.

Six different positions of the grain were taken into account.

The grain width measurements thus obtained for one of the hematite grains are given in Table II. Table III presents the data for the same grain after its reduction to magnetite. As can be seen, Feret's diameter of the grain increases from 2.77 to 2.88 mm after reduction, which corresponds to an 11% volume increase of the convex envelope of the grain.

3.1.2. Stereologic measurements

After reduction each grain was mounted in epoxy resin and consecutive layers were removed by abrading and polishing. In this way 18 consecutive cross-sections were prepared and reproducibly placed on the handle of the $x - y - z$ co-ordinatemeter. Each cross-section was analysed by means of a microscope at a magnification of $\times 500$. Three different types of

TABLE II Width of hematite grain before transformation[a]

	Width at ith position and at angle φ (mm)								
Position	0°	30°	60°	90°	120°	150°	Mean	σ^2	σ
1	3.01	3.00	2.68	2.82	2.79	2.50	2.80	0.03	0.18
2	2.68	2.60	3.03	2.63	2.85	3.14	2.82	0.04	0.20
3	2.92	2.57	2.58	2.84	2.65	2.81	2.73	0.02	0.13
4	2.80	2.59	2.66	2.59	2.47	2.82	2.66	0.02	0.12
5	2.56	2.83	3.00	2.89	2.88	2.97	2.86	0.02	0.14
6	2.42	2.55	2.94	2.66	2.84	2.94	2.73	0.04	0.20
Total population							2.77	0.03	0.18

[a] $d_{FE} = 2.77 \pm 0.06$ mm; $\sigma_{36} = 0.03$ mm.

TABLE III Width of hematite grain after transformation to magnetite[a]

	Width at ith position and at angle φ (mm)								
Position	0°	30°	60°	90°	120°	150°	Mean	σ^2	σ
1	3.03	2.96	3.06	2.89	2.77	3.12	2.97	0.01	0.12
2	2.83	2.76	2.80	2.66	3.04	3.10	2.87	0.02	0.16
3	2.47	3.03	3.11	2.79	2.90	2.93	2.87	0.04	0.21
4	2.73	3.09	3.06	2.54	2.77	2.93	2.85	0.04	0.19
5	3.03	2.95	2.73	2.85	2.77	2.76	2.85	0.01	0.11
6	2.84	3.12	3.01	2.42	2.86	2.84	2.85	0.05	0.22
Total population							2.88	0.03	0.18

[a] $d_{FE} = 2.88 \pm 0.06$ mm; $\sigma_{36} = 0.03$ mm.

TABLE IV Areas of grain components determined by stereologic analysis (grain $d_{FE} = 2.88$ mm)

Layer no.	Layer thickness (mm)	Cross-sectional area of component (mm^2)				Cross-sectional area of grain (mm^2)
		Magnetite	Hematite	Large pores	Small pores	
1	0.123	0.2992	0	0.0524	0.0324	0.3840
2	0.123	0.8000	0	0.1120	0.1040	1.0160
3	0.117	1.5529	0.0016	0.2428	0.1885	1.9858
4	0.090	1.8473	0.0020	0.2095	0.3000	2.3588
5	0.121	2.5929	0.0102	0.2688	0.3039	3.1758
6	0.134	2.5920	0.0895	0.2240	0.3392	3.2447
7	0.148	3.0385	0.0885	0.3008	0.5824	4.0102
8	0.121	3.5776	0.1233	0.2849	0.3024	4.2882
9	0.120	3.8289	0.3310	0.3169	0.4210	4.8979
10	0.152	4.2671	0.1872	0.2961	0.3887	5.1391
11	0.166	4.5248	0.1701	0.3504	0.3551	5.4004
12	0.143	4.1518	0.1085	0.5216	0.6289	5.4108
13	0.192	4.0401	0.0789	0.3537	0.4575	4.9302
14	0.318	3.2046	0.0541	0.3399	0.3839	3.9825
15	0.168	2.1273	0.0455	0.2057	0.3145	2.6930
16	0.161	1.3856	0.0497	0.1344	0.2576	1.8273
17	0.114	0.9620	0.0338	0.1256	0.1912	1.3726
18	0.132	0.237[a]	0.008[a]	0.031[a]	0.047[a]	0.324[a]

[a] Values calculated under the assumption that the proportion of grain components is the same as in layer no. 17.

measurements [15] were made:

1. Point analysis using a semi-automatic measuring system, consisting of an Axioplan-Pol microscope and of a computer controlled $x - y - z$ table. The analysis was made within a square grid. The displacement step of the table was 20 μm for the initial and final cross-sections with small area, whereas for those from the centre of the grain the displacement step was 40 μm. Using the point analysis the areas of three components on consecutive cross-sections were determined: magnetite, small and large pores.

2. Determination of grain contour, i.e. the $x - y$ co-ordinates of the edge of a grain was carried out with the same equipment. The distances between the measured points on the edge of the grain were dependent on the shape of the grain. To enable the measurements to be repeated, the contours of individual cross-sections of a grain were analysed by a Metapericolor image analyser and stored in memory.

3. Planar stereologic analysis was carried out automatically by means of a Metapericolor image analyser. It was used to determine the area of hematite on a cross-section, because its low volume fraction prevented accurate point analysis.

3.1.3. Determination of volume fractions of grain components by stereologic analysis

Volume fractions of grain components were determined by measuring the areas taken by each component on the cross-section and the total area of the cross-section. In the case of point analysis, the area taken by each component was calculated by multiplying the number of points corresponding to this component by the squared distance between the measuring points. In the planar analysis, the surface area was obtained directly from the analyser. The total surface area of the examined cross-section was a sum of areas corresponding to the components. Table IV shows the results of such measurements for a reduced hematite grain with a Feret's diameter d_{FE} of 2.88 mm.

The data listed in Table IV enable determination of the volume fraction, $\bar{V}_c'$, of each grain component as a ratio of the cross-sectional area of the component, s_c, and total area of the cross-section, S_i, after transformation

$$\bar{V}_c' = \frac{s_c}{S_i}, \quad c = 1, \ldots, 4 \tag{2}$$

For illustration, Table V lists the calculated volume fractions of grain components for a reduced grain with

TABLE V Volume fractions of grain components in successive layers of reduced grain (grain $d_{FE} = 2.88$ mm)

Layer no.	Volume fraction of grain components (%)			
	Magnetite	Hematite	Large pores	Small pores
1	77.92	–	13.65	8.44
2	78.74	–	11.02	10.24
3	78.20	0.08	12.23	9.49
4	78.32	0.08	8.88	12.72
5	81.65	0.32	8.46	9.57
6	79.88	2.76	6.90	10.45
7	75.77	2.21	7.50	14.52
8	83.43	2.88	6.62	7.05
9	78.18	6.76	6.47	8.60
10	83.03	3.64	5.76	7.56
11	83.79	3.15	6.49	6.58
12	76.73	2.01	9.64	11.62
13	81.95	1.60	7.17	9.28
14	80.47	1.36	8.53	9.64
15	78.99	1.69	7.64	11.68
16	75.83	2.72	7.36	14.10
17	73.29	2.58	9.57	14.57
18	73.15[a]	2.47[a]	9.58[a]	14.51[a]

[a] Values calculated under the assumption that the proportion of grain components is the same as in layer no. 17.

TABLE VI Volume of grain and its components determined by stereologic analysis (grain $d_{FE} = 2.88$ mm)

Layer no.	Volume of grain components (mm^3)						Total volume (mm^3)	
	Magnetite		Hematite		Pores			
	Layer	Grain	Layer	Grain	Layer	Grain	Layer	Grain
1	0.0123	0.0123	0	0	0.0035	0.0035	0.0158	0.0158
2	0.0651	0.0774	0	0	0.0179	0.0214	0.0830	0.0988
3	0.1352	0.2126	0.0001	0.0001	0.0371	0.0585	0.1724	0.2712
4	0.1528	0.3654	0.0002	0.0003	0.0423	0.1008	0.1953	0.4665
5	0.2674	0.6328	0.0007	0.0010	0.0654	0.1662	0.3335	0.7988
6	0.3474	0.9802	0.0058	0.0068	0.0761	0.2423	0.4293	1.2292
7	0.4162	1.3964	0.0132	0.0200	0.1061	0.3485	0.5355	1.7648
8	0.3998	1.7962	0.0128	0.0327	0.0884	0.4368	0.5009	2.2657
9	0.4443	2.2405	0.0263	0.0590	0.0793	0.5162	0.5499	2.8156
10	0.6150	2.8555	0.0389	0.0978	0.1081	0.6243	0.7620	3.5776
11	0.7296	3.5852	0.0296	0.1275	0.1151	0.7397	0.8747	4.4522
12	0.6202	4.2054	0.0198	0.1472	0.1314	0.8711	0.7714	5.2236
13	0.7864	4.9917	0.0179	0.1652	0.1874	1.0585	0.9917	6.2153
14	1.1493	6.1411	0.0210	0.1862	0.2439	1.3024	1.4143	7.6296
15	0.4448	6.5859	0.0084	0.1945	0.1040	1.4064	0.5572	8.1868
16	0.2807	6.8666	0.0077	0.2022	0.0732	1.4796	0.3615	8.5483
17	0.1331	6.9996	0.0047	0.2069	0.0403	1.5199	0.1781	8.7264
18	0.0738	7.0735	0.0026	0.2095	0.0243	1.5443	0.1008	8.8272
19	0.0105	7.0839	0.0004	0.2099	0.0034	1.5477	0.0143	8.8415

Feret's diameter $d_{FE} = 2.88$ mm. The data given in Table IV also make it possible to calculate the volume of the grain and the volumes of its components. Calculated values are listed in Table VI.

3.1.4. Determination of grain parameters from the contours of grain cross-sections

Fig. 3 is a graphic representation of the measured co-ordinates of points located on nine consecutive contours of the same hematite grain after reduction ($d_{FE} = 2.88$ mm). The contours of consecutive grain cross-sections have the form of broken lines joining the points located on the contour edges. The contours demonstrate great variety and complexity of grain shapes after phase transformation as well as the extent of error introduced by model assumptions of the spherical shape of reduced grains. For such irregular grains, the shape of the grain projection depends on the selected projection plane (Fig. 4a, b).

To calculate the total surface area of the cross-section, an equation was used that enabled calculating the area of a plane figure with a regular contour. If the contour is a broken line joining the points with co-ordinates, x_j, y_j, the equation has the following form

$$S_i = \frac{1}{2}\left|\sum_{j=1}^{L}(x_j, y_{j+1} - x_{j+1}, y_j)\right| \quad (3)$$

where L is a number of points with co-ordinates x_j, y_j located on a contour of the cross-section of grain, and where $x_{L+1} = x_1$; $y_{L+1} = y_1$ and $j = 1, 2, 3, \ldots L$.

The total grain cross-sectional areas, calculated from Equation 3, are shown in Table VII. Comparison of these values with the areas determined by stereologic analysis (Table IV right-hand column) indicates that the results are in good agreement (see also Table VIII).

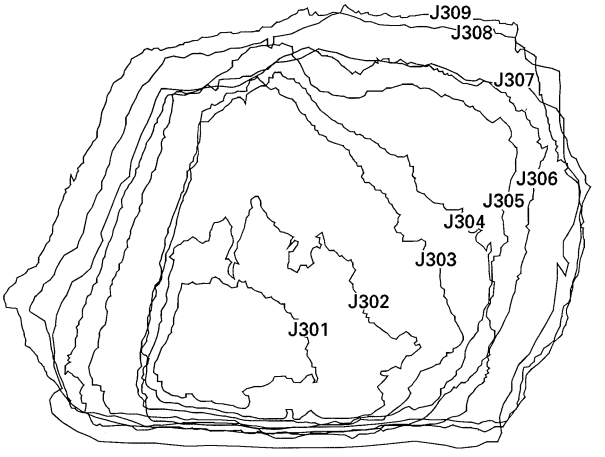

Figure 3 Contours of consecutive cross-sections (J301–J309) of a hematite grain after transformation to magnetite ($d_{FE} = 2.88$ mm).

The same set of measuring points located on a grain contour can be used for calculating the volume of a grain; however, the following simplifying assumptions must be made:

1. consecutive layers of abraded grains have the shapes of truncated cones,
2. thicknesses of extreme layers impossible to measure are equal to those of neighbouring layers.

The known thickness, h_i, of the abraded grain and the cross-sectional areas, S_i and S_{i+1}, of each consecutive layer, i, enable calculation of the volume of the layer

$$V_i' = \frac{1}{3}h_i[S_i + (\sqrt{S_i S_{i+1}})^{1/2} + S_{i+1}] \quad (4)$$

The results of these calculations for a hematite grain after reduction ($d_{FE} = 2.88$ mm) are listed in Table VII

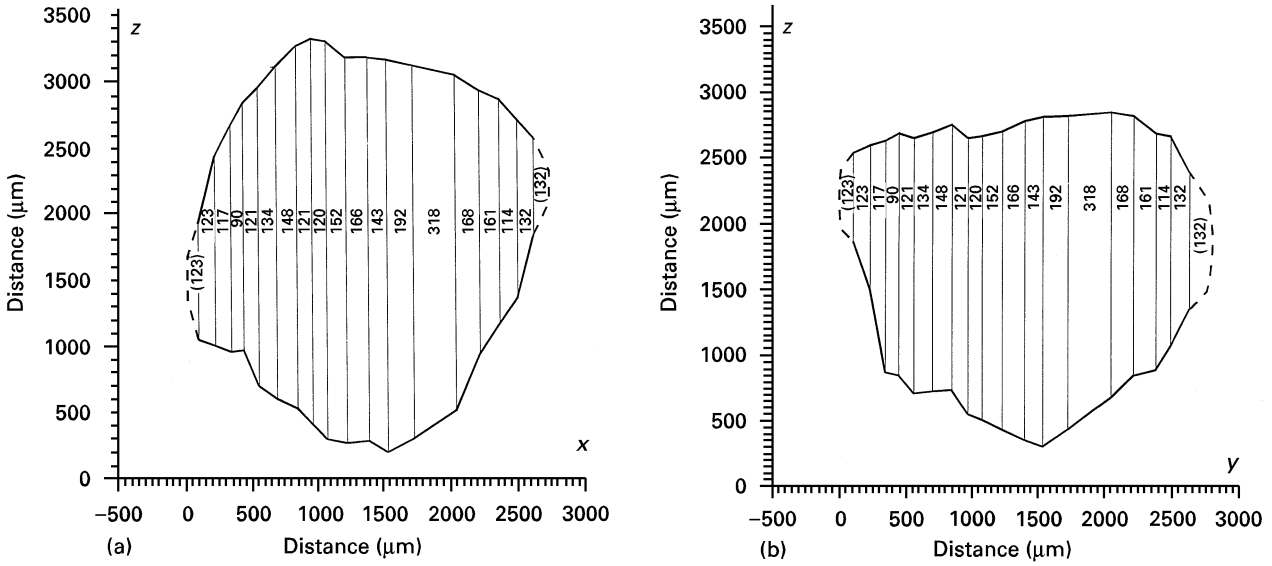

Figure 4 Projection of hematite grain after reduction to magnetite ($d_{FE} = 2.88$ mm): (a) On the xz plane, and (b) on the yz plane.

TABLE VII Cross-sectional areas and layer volumes determined by the cross-section contour method (grain $d_{FE} = 2.88$ mm) for hematite

Layer no.	Contour length (mm)	Cross-sectional area (mm^2)	Layer thickness (mm)	Volume (mm^3)	
				Layer	Grain
1	3.0446	0.3737	0.123	0.0153	0.0153
2	6.3438	0.9916	0.123	0.0809	0.0963
3	6.2901	1.9671	0.117	0.1699	0.2661
4	6.8177	2.3941	0.090	0.1959	0.4621
5	7.5380	3.1482	0.121	0.3443	0.7963
6	8.0244	3.7058	0.134	0.4587	1.2550
7	8.7327	4.3166	0.148	0.5931	1.8481
8	8.9885	4.7136	0.121	0.5462	2.3943
9	9.2430	5.0779	0.120	0.5874	2.9816
10	9.5235	5.3659	0.152	0.7936	3.7753
11	10.0538	5.5482	0.166	0.9058	4.6811
12	10.5602	5.5561	0.143	0.7940	5.4750
13	9.7806	5.0348	0.192	1.0163	6.4314
14	9.2464	4.0313	0.318	1.4386	7.9499
15	7.9598	2.7454	0.168	0.5658	8.4957
16	6.8447	1.8170	0.161	0.3647	8.8604
17	5.6168	1.1722	0.114	0.1690	9.0295
18	3.4458	0.3245	0.132	0.0930	9.1225
19	—	—	0.132	0.0143	9.1367

(the right-hand columns) give the volumes of grain layers calculated from Equation 4, and in turn, the cumulative volume of the grain after removal of layers, down to layer i. The last row in the grain volume column 6 gives the total volume of the examined grain.

The necessity of introducing simplifying assumptions may raise doubts about the usefulness of this method of calculating the volume of a grain according to Equation 4. Moreover, it is rather difficult to estimate the error of this method. It is obvious that the error becomes smaller as the thickness of removed layers decreases.

3.1.5. Definition of grain after transformation

Determination of grain volume by stereologic analysis is possible by two different methods. The total volume of a grain after reduction ($d_{FE} = 2.88$ mm) found by measuring the areas of grain components on consecutive cross-sections (Table VI, column 9) was 8.84 mm^3. In contrast to this, the volume of the grain determined by measuring the contours of consecutive cross-sections (Table VII) was 9.14 mm^3. The calculated volumes differ by 3.3%, which indicates that qualifications made in both described procedures are comparable, although this does not imply that they are totally correct. The above agreement does not exclude the occurrence of systematic error.

The porosity of a grain can be expressed as the following ratio of measured volumes

$$\varepsilon = \frac{V'_P}{V'} \tag{5}$$

where V'_P is the total volume of pores, and V' is the total volume of the grain after transformation. By

TABLE VIII Cross-sectional area of grain determined by two different methods (grain $d_{FE} = 2.88$ mm)

Layer no.	Cross-sectional area (mm^2)		Discrepancy (%)
	Cross-sectional contour method	Stereologic analysis	
1	0.3737	0.3840	− 2.76
2	0.9916	1.0160	− 2.46
3	1.9671	1.9858	− 0.95
4	2.3941	2.3588	+ 1.47
5	3.1482	3.1758	− 0.88
6	3.7058	3.2447	+ 1.44
7	4.3166	4.0102	+ 7.10
8	4.7136	4.2882	+ 9.02
9	5.0779	4.8978	+ 3.55
10	5.3659	5.1391	+ 4.23
11	5.5482	5.4004	+ 2.66
12	5.5561	5.4108	+ 2.62
13	5.0348	4.9302	+ 2.08
14	4.0313	3.9825	+ 1.21
15	2.7454	2.6930	+ 1.91
16	1.8170	1.8273	− 0.57
17	1.1722	1.3726	− 17.10
18	0.3245	0.3245	0

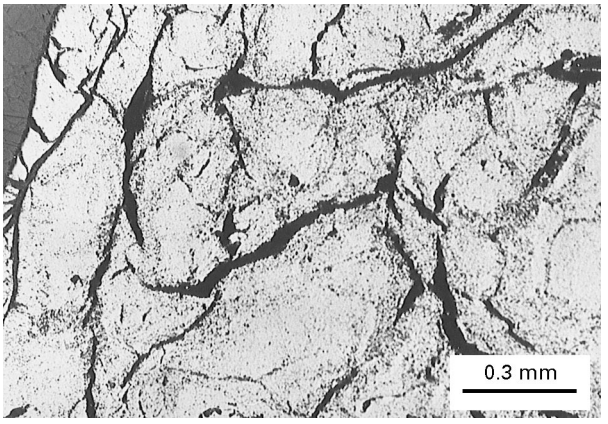

Figure 5 Cross-section of hematite grain reduced to magnetite ($d_{FE} = 2.88$ mm).

introducing the volumes determined by the above-mentioned two methods (Tables VI and VII) into Equation 5 it is possible to calculate the porosity of the grain after reduction. Thus the calculated porosity is 16.9 and 17.4%, respectively; the difference being an error of 3.6%.

In the analysis there was no problem with solid phase identification, but classification of the pores turned out to be difficult. It was intended to distinguish between the small isolated pores and interconnected larger pores and cracks. The classification was based on visual evaluation of pore size and shape (Fig. 5). Very large crack outlets near the edges of the grain were not taken into account as part of the grain (Fig. 6).

In order to illustrate the effect of assumed grain definition Table IX shows the volume of a grain after reduction ($d_{FE} = 2.88$ mm) and the volumes of the components of the grain together with the corresponding volume fractions for the three grain definitions given in Section 3.1.

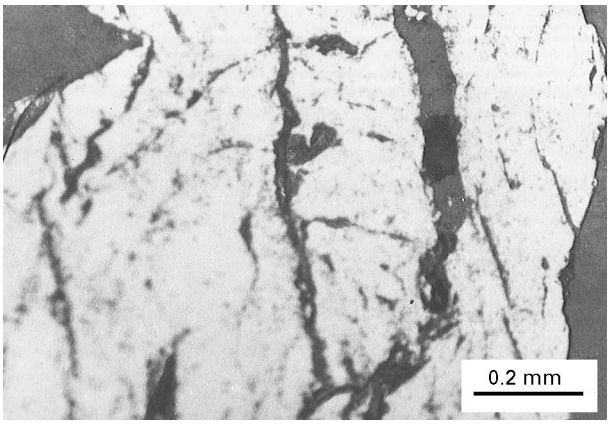

Figure 6 Crack outlet in the vicinity of the surface of the grain (Microphotograph of J301 cross-section).

Precise determination of the porosity and density of the reduced oxides is very important in describing the kinetics of the reduction process. From this point of view, the four-component definition of a grain (magnetite, hematite, small and large pores) seems the most useful and therefore it has been applied in further analysis.

3.2. Interdependence of geometric and weight parameters in a multicomponent grain

3.2.1. Density of a grain and its components

According to the adopted four-component definition of a grain (see Section 3.1.), the density of a grain after reduction, γ', can be found from the following relation

$$\gamma' = \frac{G'}{V'} = \frac{G'_H + G'_M}{V'_H + V'_M + V'_P} \quad (6)$$

where G'_H and G'_M are the weights of hematite and magnetite in the grain after transformation, and V'_H, V'_M and V'_P are the volumes of hematite, magnetite and pores, respectively, after grain transformation. G' and V' are the weight and volume of the grain after transformation. Or from an expression explicitly containing densities and volume fractions of grain components

$$\gamma' = \gamma_H \frac{\bar{V}'_H}{\bar{V}'_H + \bar{V}'_M + \bar{V}'_P} + \gamma_M \frac{\bar{V}'_M}{\bar{V}'_H + \bar{V}'_M + \bar{V}'_P} \quad (7)$$

where $\bar{V}'_H$, $\bar{V}'_M$, $\bar{V}'_P$ are the volume fractions of hematite, magnetite and pores.

Densities of the solid components of the grain (hematite, γ_H, and magnetite, γ_M) were determined independently from 3.5 g powder samples (grain sizes up to 0.1 mm) using a pycnometer: $\gamma_H = 5.257\,g\,cm^{-3}$ and $\gamma_M = 5.110\,g\,cm^{-3}$.

The weight loss during reduction was also determined

$$\frac{G' - G}{G} = \frac{0.0416 - 0.0434}{0.0434} = -4.33\% \quad (8)$$

where G was the grain weight before transformation.

TABLE IX Volumes of the grain and its components calculated according to the grain definitions 1–3 given in Section 3.1. (grain $d_{FE} = 2.88$ mm) for four, three and two components respectively

Components	Volume					
	Definition 1		Definition 2		Definition 3	
	(mm^3)	(%)	(mm^3)	(%)	(mm^3)	(%)
Magnetite	7.084	80.1	7.084	86.8	7.084	97.1
Hematite	0.210	2.4	0.210	2.6	0.210	2.9
Small pores	0.868	9.8	0.868	10.6	—	—
Large pores	0.680	7.7	—	—	—	—
Pores (total)	1.548	17.5	0.868	20.6	—	—
Grain	8.842	100.0	8.164	100.0	7.294	100.0

Equations 6 and 7 can easily be used to calculate the volumes of the grain and its components when reduction of grain is complete, i.e. $R = 1$. If, however, the reduction is partial, stereologic analysis appears indispensable.

The volumes of grains calculated from the measurements of weight and density are

1. the grain before reduction, V (hematite only, V_H)

$$V = V_H = \frac{G}{\gamma_H} = \frac{0.0434}{5.257} = 8.256\,\text{mm}^2 \qquad (9)$$

2. the grain after complete reduction (magnetite only)

$$V' = V'_M = \frac{G'}{\gamma_M} = \frac{0.0416}{5.110} = 8.141\,\text{mm}^2 \qquad (10)$$

The volume change due to the hematite–magnetite phase transformation can be calculated as

$$\frac{V'_M - V_H}{V'_M} = \frac{8.141 - 8.256}{8.141} = -1.4\% \qquad (11)$$

From the available data on densities of hematite and magnetite [16, 17] it follows that reduction results in a volume decrease of 2.2% mol^{-1} of iron. However, incorporation of iron ions into hematite during transformation of the hexagonal lattice into a regular lattice increases the volume by 11% per oxygen atom. The accompanying stresses can be relieved by plastic deformation or by crack formation. As a result the product layer will not be dense.

Based on Equations 6 and 7 it is also possible to calculate the density of the grain after reduction defined as in points 2 and 3 (see Section 3.2.). In these cases, however, it becomes necessary to take into account that the total volume of pores, V'_P, equals the volume of small pores V'_{SP} and that $\overline{V'_P} = V'_{Sp}$ or $V'_P = 0$ and $\overline{V'_P} = 0$.

3.2.2. Comparison of weight and geometric measurements

It has been found that phase transformation in the grain, selected to check the applicability of stereologic analysis, is not complete (Fig. 7). Therefore, the calculations of grain volume and density after reduction must take into account two solid phases.

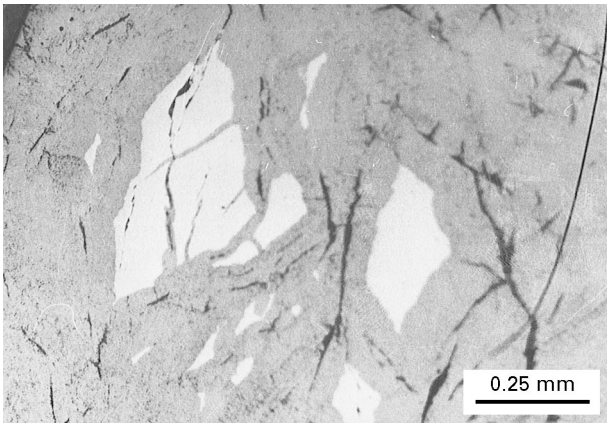

Figure 7 Cross-section J306 of reduced hematite. Grey area – magnetite and bright area – inclusions of unreacted hematite.

In Table X are listed the grain volumes $d_{FE} = 2.88$ mm, calculated from the results obtained from the different measuring methods (Equations 6 and 7), for the assumed definition of a grain.

3.2.3. Conformity criterion for determining grain volume by different methods

Grain volume can be obtained directly by a stereologic method that determines the volumes of the individual components of the grain (Table X, row 1). The volume of the grain can be also found on the basis of the known weight and density of the grain.

If the three values, i.e. V_{sterol}, G' and γ' (where V_{sterol} is the total volume of the grain after transformation determined by stereological analysis), are determined independently and error-free then the following equation should be satisfied

$$V'_{stereol} = \frac{G'}{\gamma'} \qquad (12)$$

The density measurement for a porous grain bears, however, significant error that is difficult to estimate. In this work, merely the densities of the solid grain components were measured. Grain density was

TABLE X Grain volume determined by different methods depending on assumed grain definition (see Section 3.1.), grain $d_{FE} = 2.88\,mm$[a]

Method	Volume (mm^3)		
	Definition 1	Definition 2	Definition 3
Stereological analysis	8.842	8.162	7.294
Grain weight and density of components	9.861	9.102	8.134
Volume discrepancy (%)	11.5	11.5	11.5

[a] Definition 1, four components; Definition 2, three components; Definition 3, two components.

calculated from the following equation

$$\gamma' = \gamma_H \frac{V'_H}{V'_{stereol}} + \gamma_M \frac{V'_M}{V_{stereol}} \quad (13)$$

derived directly from Equation 7, i.e. with the aid of stereologic analysis. The calculations were done for all three definitions of grain. Subsequently, the volume of the grain was determined from Equation 12. The results are shown in Table X, row 2. The application of stereologic analysis brought about a constant relative error of grain volume determination, equal to 11.5% (Table X, row 3).

If the volumes V'_H and V'_M were determined by means of stereologic analysis without any error, similarly the grain weight, G', and densities of components, γ_H and γ_M, then the relative volume difference should be zero and the following relation should be satisfied

$$G' = \gamma_H V'_H + \gamma_M V'_M \quad (14)$$

Equation 14 includes merely the volumes of solid grain components. Thus grain weight determination is not dependent on pore and crack classification or on the correctness of grain contour determination in the crack outlet. Therefore Equation 14 can be an accuracy criterion for measuring the total volume of the solid components of the grain by means of stereologic analysis at an accuracy level of weight and density measurements. This criterion becomes obvious because the grain weight is determined by weighing (left-hand side of Equation 14) or by calculating (right-hand side of Equation 14).

The criterion means that the relative difference of grain volume (and its weight), calculated by different methods, equal to 11.5%, includes measuring errors as well as errors of stereologic analysis. If the measurements were error-free then the value of 11.5% would express a limit of systematic error related to this particular method.

4. Conclusions

Application of stereologic analysis to determine the porosity of a granular material after phase transformation was aimed at obtaining more accurate and reproducible results. These results would facilitate comparison of numerous literature data. One of the advantages of this method is the determination of porosity from two independent methods of volume measurement: referring to the grain contour or volume fraction of the components of the grain. The calculated volumes differed by 3.3%. For comparison, the porosity of hematite grains partly reduced to magnetite ($R = 0.95$) was also determined by mercury porosimetry. The porosity spectrum is shown in Fig. 8. The total volume of the pores thus determined is 13.3%. Its distribution as a function of pore radius confirms the classification of pores into small ones with diameters up to 3 μm, and large ones with diameters exceeding this limit, assumed in stereologic analysis. The peaks corresponding to each type of pore are distinctly grouped in two radii ranges: micropores in the range 0.015–0.3 μm, large pores and cracks in the range 4–40 μm. The volumes related to each type of pore mentioned above amount to 10.4 and 2.2%, respectively. As can be seen in Fig. 8, pores with radii between 0.3 and 4 μm are practically of no importance.

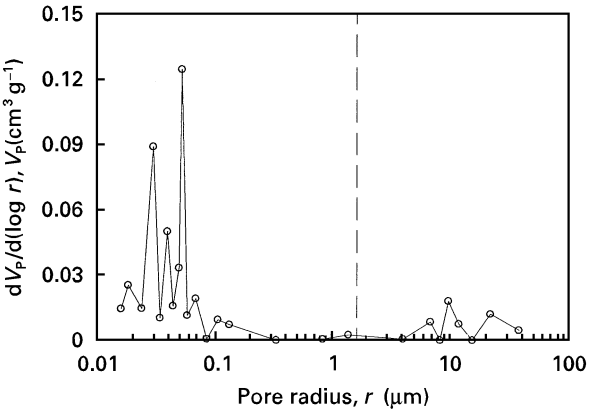

Figure 8 Porosity spectrum of hematite sample fully reduced to magnetite. (– – –) Limit between cracks and micropores assumed in stereological analysis.

Table XI shows the total porosity of the examined grain. Its value determined by a mercury method is slightly lower than that from stereologic analysis (13.3 and 17.5%, respectively). Apart from errors related to the measuring method itself this difference may be due to the presence of closed pores that are undetectable by mercury porosimetry. In both methods the volume of the micropores was determined at the same level, i.e. about 10%, which is consistent with the reported data [8, 18, 19]. For example, it has been reported by Ünal and Bradshaw [8] that at temperatures of 673–873 K the volume fraction of randomly distributed micropores with radii between 0.02 and 0.3 mm is about

TABLE XI Porosity (%) of hematite sample reduced to magnetite

	Total	Micro-pores	Cracks large pores
Porosity determined by Hg porosimetry	13.3	10.4	2.2
Porosity estimated from stereologic analysis	17.5	9.8	7.7

8.8%. The appearance of these micropores is explained by oxygen removal from the interface. Without any compensation for oxygen loss, e.g. by relaxation processes or plastic deformation, the volume fraction of pores in the magnetite phase should be 11.1%.

The difference between the results obtained in the two methods reveals in the case of large pores and cracks that cracks cannot be related to oxygen removal from the interface but rather to mechanical strains caused by localized nucleation of magnetite [10] and then disintegration of the hematite grain. Cracks form big holes near the surface of the grain that are easier to take into account in the stereologic analysis.

In spite of the mentioned discrepancies, the results obtained by the two methods can be treated as quite consistent. The stereologic analysis, although more time consuming, turned out to be more useful, particularly in cases when the amount of analysed material was small or when closed porosity was remarkable, as well as when the grains were multicomponent or partly reduced, which made it difficult to determine their densities. An additional advantage of stereologic analysis is that it enables one to determine grain volume and density as well as pore distribution and volume fractions of components on the cross-section of a grain. Such data are of great importance for the description of reduction kinetics and related phase transformations.

Acknowledgements

This work was supported by The Polish State Committee for Scientific Research under Grant No. 3 3603 91 02 during 1992–95. The authors are indebted to Professor J. Bodziony from the Strata Mechanics Research Institute, Polish Academy of Sciences, Cracow, Poland and to Mrs M. Wyderko-Delekta, DSc, from the University of Mining and Metallurgy for their interest in this study and helpful discussion.

References

1. J. JANOWSKI, A. BARAŃSKI and A. SADOWSKI, *ISIJ Int.* **36** (1996) 296.
2. S. P. TRUSHENSKI, K. LI and W. O. PHILBROOK, *Metall. Trans.* **5** (1974) 1149.
3. A. UNAL, *Trans. Inst. Min. Metall.* **95** (1986) C 179.
4. Y.-H. YANG and N. STANDISH, *ISIJ Int.* **31** (1991) 468.
5. T. SHARMA, R. C. GUPTA and B. PRAKASH, *ibid.* **31** (1991) 312.
6. M. JALLOULI and F. AJERSCH, *J. Mater. Sci.* **12** (1986) 3528.
7. M. OTTOW, PhD thesis, Technische Hochschule, Berlin (1966).
8. A. ÜNAL and A. V. BRADSHAW, *Metall. Trans. B* **14B** (1983) 743.
9. R. L. BLEIFUSS, *Trans. Soc. Min. Engrs. AIME*, **247** (1970) 225.
10. F. ADAM, B. DUPRE and C. GLEITZER, *React. Solids* **5** (1988) 101.
11. J. JANOWSKI, A. SADOWSKI, M. WYDERKO-DELEKTA and J. DELEKTA, *Metall. Foundry Eng.* **20** (1994) 161.
12. M. ETTABIROU, B. DUPRE and C. GLEITZER, *React. Solids* **5** (1988) 306.
13. J. JANOWSKI, M. WYDERKO-DELEKTA, A. SADOWSKI and J. DELEKTA, *Solid State Phenom.* **41** (1995) 55.
14. J. BODZIONY, *Bull. Acad. Polon. Sci., Ser. IV* **12** (1965) 883.
15. *Idem*, *ibid.* **12** (1965) 793.
16. R. DIECKMANN, H. SCHMALZRIED and T. O. MASON, *Arch. Eisenhüttenwess*, **52** (1981) 211.
17. J. JANOWSKI, Unpublished work.
18. A. BRADSHAW and A. G. MATYAS, *Metall. Trans. B* **7B** (1976) 81.
19. H. BRILL-EDWARDS, B. L. DANIELL and R. L. SAMUEL, *JISI* **203** (1965) 361.

Received 19 April 1996
and accepted 8 July 1997